



Contents lists available at ScienceDirect

Spectrochimica Acta Part A: Molecular and Biomolecular Spectroscopy

journal homepage: www.elsevier.com/locate/saa

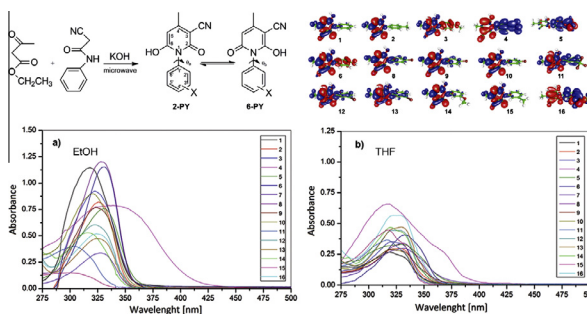
Solvent and structural effects in tautomeric 2(6)-hydroxy-4-methyl-6(2)-oxo-1-(substituted phenyl)-1,2(1,6)-dihydropyridine-3-carbonitriles: UV, NMR and quantum chemical study

Ismail Ajaj^a, Jasmina Markovski^b, Milica Rančić^{c,*}, Dušan Mijin^a, Miloš Milčić^d, Maja Jovanović^d, Aleksandar Marinković^a^a Faculty of Technology and Metallurgy, University of Belgrade, Karnegijeva 4, 11120 Belgrade, Serbia^b Vinča Institute, University of Belgrade, 11000 Belgrade, Serbia^c Faculty of Forestry, University of Belgrade, Kneza Višeslava 1, 11030 Belgrade, Serbia^d Faculty of Chemistry, University of Belgrade, Studentski trg 3–5, 11000 Belgrade, Serbia

HIGHLIGHTS

- The tautomeric equilibria of title molecules are investigated experimentally and theoretically.
- Influence of solvent and substituent on UV–vis absorption spectra was examined.
- K_T values of the investigated compounds were determined.
- ICT process was deduced from Bader's analysis.

GRAPHICAL ABSTRACT



ARTICLE INFO

Article history:

Received 29 August 2014

Received in revised form 12 May 2015

Accepted 13 May 2015

Available online 6 June 2015

Keywords:

Tautomerism

Solvent effects

Substituent effects

DFT

Derivative spectroscopy

ABSTRACT

The state of the tautomeric equilibria of 2(6)-hydroxy-4-methyl-6(2)-oxo-1-(substituted phenyl)-1,2(1,6)-dihydropyridine-3-carbonitriles, **2-PY/6-PY**, was evaluated using experimental and theoretical methodology. The experimental data were interpreted with the aid of time-dependent density functional (TD-DFT) method. Electron charge density was obtained by the use of Quantum Theory of Atoms in Molecules, *i.e.* Bader's analysis. Linear solvation energy relationships (LSER) rationalized solvent influence on tautomeric equilibrium. Linear free energy relationships (LFERs) were applied to the substituent-induced NMR chemical shifts (SCS) using SSP (single substituent parameter) and DSP (dual substituent parameter) model. Theoretical calculations and obtained correlations gave insight into the influence of molecular conformation on the transmission of substituent electronic effects, as well as on different solvent–solute interactions, and the state of tautomeric equilibrium.

© 2015 Elsevier B.V. All rights reserved.

Introduction

2-Pyridones are important heterocyclic compounds widely used in medicinal chemistry, and their various derivatives have

significant biological activity. They can possess antibacterial, anti-fungal, anti-inflammatory, antiviral, antitumor and antiplatelet properties [1]. In addition, they are used in the manufacturing of paints, pigments, additives for fuels and lubricants, acid-base indicators, stabilizers for polymers and coatings [2]. Many medications containing 2-pyridone structure are cardiotonics: Milrinone and Amrinone; antibiotics: Pilicides and Curlicides, and antiepileptic: Perampanel [1].

* Corresponding author. Tel.: +381 11 3053 893; fax: +381 11 2547 478.

E-mail address: milica.rancic@sfb.bg.ac.rs (M. Rančić).

In general, 2(1H)-pyridones exhibit keto-enol or 2-pyridone (PY)/2-hydroxypyridine (HP) (lactam/lactim) tautomerism. The small free energy difference between tautomers makes them sensitive to the influence of environment (e.g. pH, temperature, solvent polarity and the ability of solvents to hydrogen bond with each tautomer), substituent effects (their position in the ring and their electronic effects, and inter- and intramolecular interactions [3]. Therefore, it is important to evaluate the potential for tautomerization in heteroaromatic systems and to assess the role of individual tautomers in biological activity. In this context, using the cardiotoxic agent Milrinone as the template, structure–property and structure–activity relationships of several series of differently substituted 2(1H)-pyridones have been investigated. It has been shown that their lipophilicity (expressed as octanol–water partition coefficient, log *P*) significantly depends on the tautomerism [4] i.e. “hydroxy” (HP) tautomer should be at least 20-fold more lipophilic than the respective “oxo” (PY) tautomer. Lipophilicity is directly related to the change in the Gibbs energy of a solute solvation between octanol and water; solute dipolarity/polarizability and, especially, solute hydrogen bond basicity favors partitioning into water and thus decreases lipophilicity, while solute size favors octanol [5]. Because of this, solvation characteristics of the corresponding tautomeric forms need to be taken into account for an accurate estimation of their pharmacologically-relevant properties.

Due to diversity of their physico-chemical properties and biological effects, tautomerism of 2(1H)-pyridones was extensively studied from both experimental and theoretical point of view: UV–Vis [6,7], infra-red [8–10], nuclear magnetic resonance [7,11–13], gas-phase [8,14–16], theoretical [16–19] and crystallographic studies [7,20–21]. These studies have shown that the pyridone form predominates in polar solvents and the solid [6,7,12], while in non-polar solvents both tautomers can co-exist [7]. Other studies showed that there is an existence of an equilibrium mixture of two tautomers in the solid, liquid and vapor phases [10,14]. Theoretical studies based on different methods have been used to calculate the tautomerization energy for lactim/lactam and similar heterocyclic systems. Geometry optimization, rotational constants, dipole moments, relative electronic energies, solvation energy, tautomerization constants, have been recognized as important data to these and related isomerization reactions [22–25].

In this work, linear solvation and free energy relationships, LSER and LFER, respectively, and quantum-chemical calculations of recently synthesized 2(6)-hydroxy-4-methyl-6(2)-oxo-1-(substituted phenyl)-1,2(1,6)-dihydropyridine-3-carbonitriles (Fig. 1) [25], were performed.

Quantification of the solvent effects: dipolarity/polarizability and the hydrogen-bonding ability on the UV spectral shifts were interpreted by means of the Kamlet–Taft (LSER) Eq. (1) [26]:

$$\nu = \nu_o + s\pi^* + b\beta + \alpha\alpha \quad (1)$$

where π^* is an index of the solvent dipolarity/polarizability; α is a measure of the solvent hydrogen-bond acceptor (HBA) basicity; β is a measure of the solvent hydrogen-bond donor (HBD) acidity

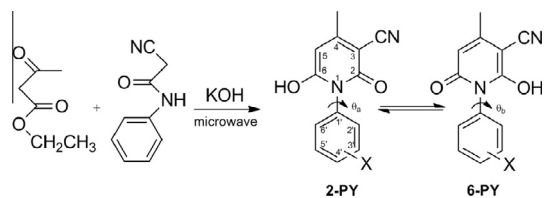


Fig. 1. Microwave assisted synthesis of tautomeric **2-PY** and **6-PY** pyridones, where X is: H (1); 4-CH₃ (2); 4-OCH₃ (3); 4-NO₂ (4); 4-COCH₃ (5); 4-OH (6); 4-I (7); 4-Cl (8); 4-Br (9); 4-F (10); 3-CF₃ (11); 3-Cl (12); 3-Br (13); 3-OCH₃ (14); 3-CH₃ (15); 3-COCH₃ (16).

and ν_o is the regression value in cyclohexane as reference solvent. The solvent parameters used in Eq. (1) are given in Table S1. The regression coefficients *s*, *b* and *a* in Eq. (1) measure the relative susceptibilities of the absorption frequencies to the different solvent parameters.

More elaborated LSER model uses Catalán solvent parameters scale [27,28], i.e. Eq. (2) which qualitatively and quantitatively interprets the effect of solvent dipolarity, polarizability and solvent–solute hydrogen bonding interactions according to Eq. (2):

$$\nu = \nu_o + aSA + bSB + cSP + dSdP \quad (2)$$

where SA, SB, SP and SdP characterize solvent acidity, basicity, polarizability and dipolarity, respectively (Table S2). The regression coefficients *a–d* describes the sensitivity of the absorption maxima to different types of the solvent–solute interactions.

In the second part of the work, LFER analysis was applied to the UV and SCS data in the studied compounds (Fig. S1). The transmission of polar (field/inductive) and resonance effects from the substituent (X) to the carbon atoms of interest were studied using Eqs. (3) and (4):

$$s = \rho\sigma + h \quad (3)$$

$$s = \rho_I\sigma_I + \rho_R\sigma_R + h \quad (4)$$

where *s* are substituent-dependent values: SCS or absorption frequencies (ν); ρ is a proportionality constant (reaction constant) reflecting the sensitivity of the spectral data to the substituent effects; σ , σ_I and σ_R are the substituent constants (Table S3), and *h* is the intercept (i.e. it describes the unsubstituted member of the series) [29]. Single substituent parameter Eq. (3) (SSP; the Hammett Equation) attributes the observed substituent effect to an additive blend of polar and π -delocalization effects given as corresponding the σ values. In the dual-substituent parameter (DSP) Eq. (4) (the Extended Hammett Equation), *s* are correlated by a linear combination of inductive (σ_I) and various resonance scales (σ_R^0 , σ_R^- and σ_R^+), depending on the electronic demand of the atom under study. Calculated values ρ_I and ρ_R , are relative measures of the transmission of the inductive and resonance effects.

Experimental and theoretical data of both tautomeric forms are considered. The UV–Vis and NMR data were analyzed by the use of LSER and LFER models, respectively, in order to evaluate influences of solvent/solute interactions and substituent effects on tautomeric equilibria and the extent of ICT. Due to overlapping of the absorption bands, applied methodology for resolution of UV–Vis spectra was based on certain approximations [30]. The algorithm applied for evaluation of the state of tautomeric equilibria was described elsewhere [25,31]. A thorough study of the relative stability of tautomers typically requires the use of computational techniques to supplement the experimental findings. Geometries of compounds were optimized by DFT calculations. Time-dependent density functional theory (TD-DFT) calculation was applied for estimation of the transition energy. TD-DFT was successfully applied for description of solvated organic molecules with a possibility of estimation of electronic density transfer [32], and the influence of molecular geometry on ICT [33]. The transmission of substituent effects, i.e. LFER study, was discussed in relation to the geometry of molecules (DFT) and the charge distribution analysis (Bader's analysis).

Material and methods

Materials

All used materials and solvents (UV spectrophotometric grade) were obtained commercially (Fluka and Sigma–Aldrich), and used without purification.

Synthesis and characterization of tautomeric pyridone products

Synthesis of 2(6)-hydroxy-4-methyl-6(2)-oxo-1-(substituted phenyl)-1,2(1,6)-dihydropyridine-3-carbonitriles was described in the previous study [25]. Detail on FTIR and NMR characterization methods is provided in [Supplementary material](#).

The UV absorption spectra were recorded in the range from 200 to 600 nm in sixteen solvents of different polarity using UV-Vis Shimadzu 1700A spectrophotometer. Spectra were recorded at variable conditions, temperature and concentration, as well as solvent mixtures, to study their effect on the tautomeric equilibria. Concentration was changed in the range from 1.00×10^{-4} to 1.00×10^{-7} mol dm⁻³, and at temperature of 25, 35, 45 and 55 ± 0.1 °C (Fig. S1). The constant $K_T = [6\text{-PY}]/[2\text{-PY}] ([b]/[a])$ was calculated as the ratio of the estimated area of the corresponding tautomeric form.

Molecular geometry optimization and theoretical absorption spectra calculation

The ground state geometries of compounds **1–6** and **8–16** were fully optimized with DFT method, more specifically the Becke three-parameter exchange functional (B3) and the Lee–Yang–Parr correlation functional (LYP) with 6-311G(d,p) basis set without symmetry constrain, and with default tight convergence criteria. Because no adequate basis set was found for Iodine atom, compound **7** was excluded from computational consideration. Global minima were found for each optimized compound. Harmonic vibrational frequencies have been evaluated at the same level to confirm the nature of the stationary points found (to confirm that optimized geometry corresponds to minimum that has only real frequencies), and to account for the zero point vibrational energy (ZPVE) correction. The frontier molecular orbital energies: E_{HOMO} for highest occupied molecular orbital (HOMO) and E_{LUMO} for lowest unoccupied molecular orbital (LUMO) and HOMO–LUMO energy gaps (E_{gap}) were calculated with B3LYP/6-311G(d,p) method on gas phase optimized geometries. Theoretical absorption spectra of both tautomeric forms were calculated in gas phase, ethanol, tetrahydrofuran and dimethylsulfoxide with TD-DFT method. For TD-DFT calculations solvents have been simulated with standard static isodensity surface polarized continuum model (IPCM) [34].

NMR chemical shifts are calculated on the optimized structures using GIAO calculations in chloroform as a solvent, with the specially parameterized WP04 [35] functional using cc-pVDZ basis set. This method was proven to give best accuracy/cost ratio in NMR chemical shift prediction, and was invoked in Gaussian program by method prescribed by Jain, Bally and Rablen [36]. The values of ¹³C chemical shifts presented in [Tables S4 and S5](#)

are scaled relative to ¹³C chemical shift of TMS, calculated with the same method. Solvent in NMR calculations was simulated with Polarizable Continuum model (PCM). Good agreement of calculated and experimental NMR value was obtained (Fig. S2). All calculations were done with Gaussian09 software [37].

The Bader's analysis were done on charge density grid with program “Bader” [38]. The ground state and excited state electron densities were calculated on ground state optimized geometries with B3LYP/6-311(d,p) method. Density difference maps were plotted as difference between electron densities of the first excited state and the ground state, in program gOpenMol [39].

Results and discussion

Resolution of UV spectra. Solvent effects on the state of 2-PY/6-PY equilibrium

Pyridones could exist in a solution as the equilibrium of tautomeric forms and eventually dimer forms [39,40]. This phenomenon has significant influence on physico-chemical properties of the studied pyridones. Tendency of 2-pyridone to aggregate was evaluated from NMR and FTIR spectral data [39]. State of tautomeric equilibrium sensitively depends on solvent properties like polarity, stabilization of the charges in the solvation sphere and alteration of a solute's electronic structure in the ground and excited state due to both short- and long-range interactions with surrounding solvent molecules [25,41]. Additionally, geometries and substituent effects could be of appropriate significance.

Various spectroscopic techniques were applied for studying the state of tautomeric equilibria, mechanism of proton-transfer and solvent–solute interactions [42–44]. The rate of prototropic exchange depends on energetic phenomena, *i.e.* transformation barrier, system parameters and environment. Slow proton exchange allows observation of distinct signals in ¹H NMR spectra and quantitative determination of the tautomeric forms [25]. Oppositely, under fast proton exchange in tautomeric mixture, only one, average, signal in the NMR spectrum was observed. UV-Vis technique is a useful method for study of tautomeric equilibrium which could be based on the following advantages: different spectral properties of tautomeric forms, tautomeric equilibria sensitivity to environment (solvent), substituent effect, acidity, temperature, *etc.* Accordingly, state of the tautomeric equilibria, influences of substituent effect and geometry of investigated compounds **1–16** were studied by analyzing UV-Vis spectra [45]. Absorption spectra of the investigated compounds, recorded in sixteen solvents, showed that spectra consist of two overlapped bands in the region 300–500 nm (Fig. 2). The band structure depends on both substituent effects and solvent properties.

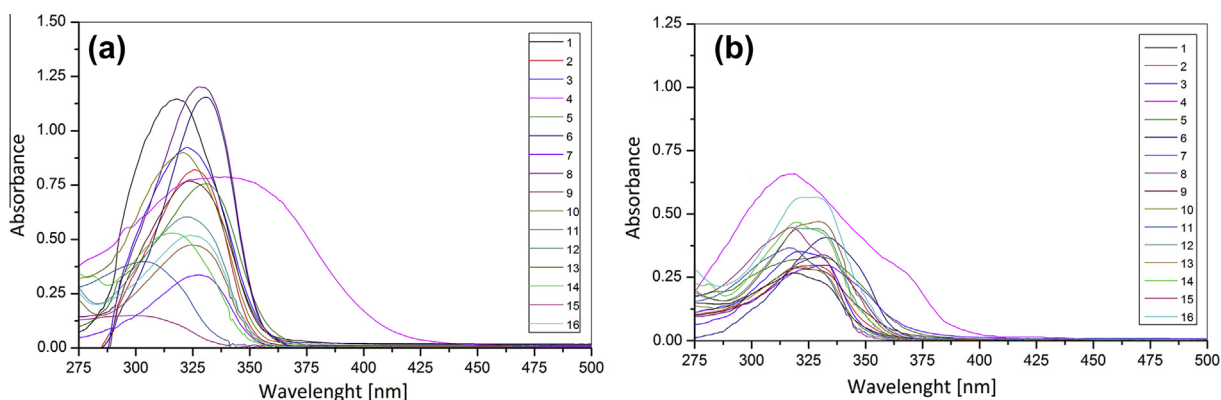


Fig. 2. Absorption spectra of compounds **1–16** in (a) ethanol and (b) THF.

Dimerization process was not observed at concentration lower than $1 \times 10^{-5} \text{ mol dm}^{-3}$, indicating no monomer content rising upon dilution. Therefore, all UV–Vis spectra were recorded at concentration of $1 \times 10^{-5} \text{ mol dm}^{-3}$. The characteristic absorption spectra of investigated compounds in ethanol and THF are shown in Fig. 2.

A semi quantitative approach was applied for the analysis of the state of tautomeric equilibria. The spectra were analyzed by a stepwise procedure, whereby an estimation of tautomerization constants, individual spectra of the tautomers and absorption bands numbers were obtained from both experimental data and TD-DFT calculation. The second and fourth derivative spectroscopy are useful methodologies for determining the number and approximate position of the absorption bands [25,45]. In the second step, the initial approximation of the band intensities and band widths, as well as the assignment to the appropriate tautomeric form were performed. The final refinement is performed by simultaneous resolution of the whole set of spectra according to literature procedures [25,29,30,46]. TD-DFT calculations have shown (Tables S6 and S7; Figs. S3 and S4) that **2-PY** form will have absorption maxima on higher wavelength (lower energy) than **6-PY** form in all investigated solvents as well as in gas phase. The results of the applied methodology are exemplified in Fig. S5. Absorption maxima of both **2-PY** and **6-PY** forms obtained in the set of selected solvents are summarized in Tables 1 and S8, respectively. Such methodology provides differentiation without loss of the terminal spectral points [47].

The absorption band maxima could be assumed to be mainly π – π^* transition involving the π -electronic system throughout the whole molecule including ICT. The considerable ICT nature of this band is obvious from its broadness, the sensitivity of its λ_{max} to the substituent effects and the solvent properties. The data from Table 1 confirm that the positions of the UV–Vis absorption frequencies depend on the nature of the present substituent on the benzene ring. The introduction of both electron-donating and electron-withdrawing substituents contributes to the positive solvatochromism, comparing to the unsubstituted compound, except for compounds **5**, **11** and **15**. The absorption spectra showed relatively low dependence on both solvent and substituent effects for **2-PY** tautomer (Table 1), and somewhat higher influence was observed for **6-PY** tautomer (Table S8). Solvent dependent spectral shifts are influenced by non-specific (dipolarity/polarizability) and specific (HBA/HBD) solvent–solute interactions. Generally, tautomeric equilibrium is shifted to more dipolar form with increasing solvent polarity [48].

LSE analysis of UV data

The contribution of specific and nonspecific solvent–solute interactions was quantitatively evaluated by the use of LSE Eqs. (1) and (2). The LSE concepts developed by Kamlet and Taft and Catalán are some of the most successfully used for quantitative treatments of solvation effects [48]. This treatment assumes attractive/repulsive solvent/solute interactions and enables an estimation of the ability of the solvated compounds to interact with solvent. Correlation results obtained by the use Kamlet–Taft and Catalán model are given in Tables 2 and 3 for **2-PY** form, and S9 and S10 for **6-PY** form, respectively.

The percentages contribution of the nonspecific (P_{π}) and the specific solvent/solute interactions (P_{β} and P_{α}) are given in Tables S11 and S12.

The positive values of the coefficient a obtained for both **2-PY** and **6-PY** forms, except for compounds **5**, **8** and **11** in **6-PY** form, indicate better stabilization of the molecule in the ground state (Tables 2 and S9). It implies that proton-accepting capabilities of both pyridone nitrogen and keto/hydroxy group contribute in moderate/high extent to the solute stabilization in ground state. The highest values of coefficient a were found for compound **11** in both **2-PY** and **6-PY** forms.

A negative sign of the coefficients s and b , obtained in correlations for compounds in **2-PY** form, except for compounds **12–15**, for non-specific solvent effect (Table 2), indicates a bathochromic shift of the absorption maxima with the increasing contribution of solvent dipolarity/polarizability and hydrogen-accepting capability. The largest value of coefficient s (-3.29) and b (-7.51) (Table 2) was found for compound **4** in **2-PY** form. It means that the most effective transmission of the substituent effect, i.e. electron-accepting ability of the nitro group (comp. **4**), from *para*-position to the pyridone ring cause higher susceptibility of electronic density to solvent dipolarity/polarizability and hydrogen-bonding ability, i.e. higher value of coefficients s and b was obtained. Conversely, positive sign of the coefficients s and a , obtained for **6-PY** form (Table S9; except for comps. **3–5**, **8** and **9** – coefficient s ; and compounds **2**, **13** and **16** – coefficient b), indicates hypsochromic shift in relation to increased contribution of the non-specific and HBD solvent effects. Complex influences of solvent effects on ν_{max} shift were observed for both forms, while solvent effect on UV–Vis absorption maxima of the compounds in **6-PY** form could be interpreted as inconsistent alteration of correlation parameters with respect to solvent effect (Tables 2 and S9).

Table 1
Absorption frequencies of **2-PY** tautomer in selected solvents.

Solvent/compound	$\nu_{\text{max}} \times 10^{-3} \text{ (cm}^{-1}\text{)}$															
	1	2	3	4	5	6	7	8	9	10	11	12	13	14	15	16
Ethanol	31.25	30.67	30.96	29.85	31.26	30.21	30.49	30.49	30.96	31.15	32.34	30.41	30.19	30.72	31.55	30.19
Methanol	31.55	30.86	31.25	29.85	31.63	30.49	30.49	30.86	31.25	31.25	32.26	30.34	30.56	30.87	31.62	30.11
2-Propanol	31.95	30.49	31.06	28.82	31.24	30.12	30.30	30.39	30.86	31.06	31.43	30.17	29.96	31.11	31.51	29.96
1-Propanol	31.35	30.67	30.77	28.40	30.98	30.39	30.30	30.30	30.49	31.06	32.09	30.11	30.11	30.72	31.43	30.41
1-Butanol	31.45	30.58	31.06	28.57	31.50	30.30	30.30	30.30	30.77	31.15	31.27	30.04	29.96	30.72	31.75	30.34
2-Butanol	31.35	30.39	30.96	28.41	31.23	30.21	30.21	30.30	30.77	30.96	31.72	29.97	30.10	30.71	31.35	30.10
DMSO	29.95	29.74	29.72	27.24	29.99	29.52	29.66	29.65	29.74	30.03	– ^a	29.87	29.73	30.73	30.71	29.86
Tetrahydrofurane (THF)	31.45	30.39	31.15	31.15	31.43	30.03	30.21	30.21	30.93	31.25	30.85	29.77	30.17	30.64	30.99	30.03
Acetonitrile (AcN)	31.25	30.39	30.77	31.54	31.00	29.94	30.39	30.30	30.92	30.86	30.57	30.10	29.90	30.37	31.30	29.97
Anisole	31.06	30.96	31.06	31.35	31.20	30.58	30.77	30.67	30.96	31.06	30.22	30.04	28.85	30.04	30.28	30.01
Dimethylacetamide DMAc)	30.58	30.03	30.39	30.58	30.54	29.59	29.76	29.76	30.30	30.39	31.15	30.16	29.81	30.16	31.08	30.04
Dimethylformamide (DMF)	30.03	29.59	30.03	26.88	30.22	29.67	29.41	29.50	29.50	29.76	29.23	29.04	29.16	29.83	30.58	29.01
Ethyl acetate (EtAc)	31.35	30.39	31.15	31.75	31.42	30.03	30.21	30.49	30.49	31.25	30.40	29.75	29.69	30.43	30.53	29.97
Chloroform (Chl)	31.68	30.95	31.00	32.00	31.21	30.45	30.98	30.85	31.36	31.35	32.24	30.31	30.60	30.81	31.45	30.06
Dioxane	31.40	30.54	31.25	31.21	31.45	30.05	30.15	30.66	30.89	31.31	32.03	29.70	29.50	30.31	30.41	30.21
Diethyl ether (DEE)	31.50	30.74	31.36	31.00	31.56	30.14	30.06	30.51	30.95	31.42	31.56	29.58	29.31	30.15	30.14	30.15

^a Tautomer **6-PY** predominates.

Table 2Correlation results of the **2-PY** form obtained according to the Kamlet–Taft equation.

Comp.	$\nu_0 \times 10^{-3}$ (cm^{-1})	$s \times 10^{-3}$ (cm^{-1})	$b \times 10^{-3}$ (cm^{-1})	$a \times 10^{-3}$ (cm^{-1})	R^a	Sd^b	F^c	Solvent excluded from correlation
1	32.69 ± 0.25	-1.83 ± 0.34	-0.97 ± 0.26	0.46 ± 0.19	0.93	0.22	23.45	2-Propanol
2	31.33 ± 0.17	-1.00 ± 0.23	-0.81 ± 0.18	0.55 ± 0.13	0.94	0.15	26.48	Anisole
3	32.53 ± 0.22	-1.79 ± 0.30	-1.05 ± 0.22	0.28 ± 0.16	0.93	0.19	27.11	–
4	36.10 ± 1.01	-3.29 ± 1.24	-7.51 ± 1.40	0.78 ± 0.40	0.91	0.77	16.59	DMAC, Chl
5	32.81 ± 0.27	-1.75 ± 0.34	-1.23 ± 0.37	0.46 ± 0.22	0.92	0.22	20.37	Chl
6	30.59 ± 0.09	-0.66 ± 0.13	-0.52 ± 0.10	0.56 ± 0.07	0.97	0.08	54.71	Anisole
7	30.81 ± 0.17	-0.36 ± 0.23	-1.10 ± 0.18	0.77 ± 0.13	0.93	0.15	25.28	Anisole
8	31.32 ± 0.20	-0.95 ± 0.27	-1.02 ± 0.20	0.53 ± 0.15	0.92	0.17	21.42	Anisole
9	31.94 ± 0.29	-1.17 ± 0.39	-1.46 ± 0.29	0.84 ± 0.22	0.91	0.24	16.36	THF, Anisole
10	32.55 ± 0.22	-1.79 ± 0.30	-1.03 ± 0.26	^d	0.92	0.21	23.14	–
11	33.06 ± 0.49	-2.96 ± 0.67	-1.74 ± 0.14	2.12 ± 0.31	0.95	0.34	27.78	DMAC, Dioxane
12	29.49 ± 0.14	0.81 ± 0.19	-0.33 ± 0.14	0.69 ± 0.10	0.91	0.12	17.09	DMF
13	29.56 ± 0.23	0.70 ± 0.30	-0.87 ± 0.23	1.19 ± 0.17	0.91	0.19	16.43	THF, Anisole
14	29.70 ± 0.21	0.40 ± 0.25	0.82 ± 0.29	0.31 ± 0.17	0.91	0.15	13.73	THF, DMF, Chl, DMAC
15	30.30 ± 0.28	0.48 ± 0.20	–	1.41 ± 0.21	0.93	0.24	20.16	AcN, Chl
16	32.47 ± 0.39	-2.95 ± 0.49	-1.21 ± 0.34	0.30 ± 0.20	0.94	0.16	16.59	DMAC, DMSO, Chl, 2-Butanol, DEE

^a Correlation coefficient.^b Standard deviation.^c Fisher test of significance.^d Negligible values with high standard errors.**Table 3**Results of the correlation analysis for **2-PY** tautomer according to Catalán equation.

Comp.	$\nu_0 \times 10^{-3}$ (cm^{-1})	$c \times 10^{-3}$ (cm^{-1})	$d \times 10^{-3}$ (cm^{-1})	$b \times 10^{-3}$ (cm^{-1})	$a \times 10^{-3}$ (cm^{-1})	R^a	Sd^b	F^c	Solvent excluded from correlation
1	35.12 ± 0.93	-3.65 ± 1.24	-1.39 ± 0.37	-0.94 ± 0.39	0.87 ± 0.49	0.90	0.28	10.41	2-Propanol
2	32.23 ± 0.59	-0.82 ± 0.78	-1.17 ± 0.23	-0.99 ± 0.24	1.43 ± 0.31	0.92	0.18	15.72	–
3	34.40 ± 0.64	-3.15 ± 0.85	-1.47 ± 0.25	-0.60 ± 0.26	0.57 ± 0.34	0.93	0.19	18.23	–
4	43.13 ± 2.56	-10.62 ± 3.34	-3.27 ± 1.06	-5.99 ± 1.04	-0.84 ± 1.37	0.93	0.75	15.52	DMAC
5	34.70 ± 0.68	-3.27 ± 0.91	-1.49 ± 0.27	-0.58 ± 0.28	0.79 ± 0.36	0.93	0.21	17.45	–
6	30.89 ± 0.41	^d	-1.19 ± 0.18	-0.60 ± 0.17	1.43 ± 0.22	0.95	0.12	21.85	Dioxane
7	31.74 ± 0.69	–	-0.89 ± 0.32	-1.53 ± 0.31	1.98 ± 0.47	0.91	0.20	11.11	Methanol, Dioxane
8	32.59 ± 0.46	-1.37 ± 0.61	-1.15 ± 0.18	-1.15 ± 0.19	1.27 ± 0.24	0.95	0.14	28.29	–
9	33.74 ± 0.92	-2.36 ± 1.23	-1.00 ± 0.37	-1.66 ± 0.411	1.48 ± 0.51	0.90	0.28	9.61	THF, 2-Butanol
10	34.37 ± 0.72	-2.78 ± 0.96	-1.59 ± 0.29	-0.77 ± 0.29	0.83 ± 0.38	0.92	0.22	15.76	–
11	29.08 ± 1.37	–	-0.96 ± 0.50	1.21 ± 0.55	2.56 ± 0.60	0.94	0.32	15.76	Chl, DMF
12	28.73 ± 0.49	1.27 ± 0.60	0.67 ± 0.18	-0.34 ± 0.17	0.94 ± 0.21	0.92	0.11	13.42	DMF, DMSO
13	30.54 ± 0.77	-2.90 ± 1.06	1.03 ± 0.37	0.44 ± 0.39	0.98 ± 0.43	0.91	0.23	10.04	THF, Chl, Dioxane
14	29.67 ± 0.55	–	0.62 ± 0.25	0.90 ± 0.27	–	0.90	0.16	9.07	DMF, DMAC, Chl
15	32.69 ± 0.65	-2.34 ± 0.93	-0.95 ± 0.26	-0.64 ± 0.25	1.22 ± 0.34	0.92	0.18	14.50	Anisole
16	28.75 ± 1.13	2.30 ± 1.47	-1.84 ± 0.44	0.89 ± 0.51	1.89 ± 0.56	0.90	0.21	6.03	DMAC, THF, EtAc, AcN, Chl

^a Correlation coefficient.^b Standard deviation.^c Fisher test of significance.^d Negligible values with high standard errors.

Quantitative separation of the non-specific solvent effect (coefficient s ; Tables 2 and S9) into polarizability and dipolarity term (coefficients c and d , Tables 3 and S10) point out to more pronounced influence of the solvent polarizability on stabilization of the excited state in both forms (except comps. 12 and 16, coefficient c ; and comps. 12–14, coefficient d in **2-PY** form; Table 3). An exception for compounds 6, 7 and 11 in **2-PY** form, with highest values of coefficient a was observed. Inconsistent alternation of the sign of coefficients c and d was found for compounds in **6-PY** form (Table S9). Significant number of compounds shows negligible values of non-specific and HBA solvent effects on ν_{max} shift of the investigated compounds in **6-PY** form (Table S9). The highest value of coefficient c found for compound 4 in **2-PY** form and significantly lower in **6-PY** form indicate that strong electron-withdrawing character of the nitro group causes the higher extent of π -electron delocalization which contributes to larger π -electron polarizability in **2-PY** form. This could not be applied for compounds in **6-PY** form where the pronounced non-specific solvent effect was observed for compounds 4, 6 and

11, showing that both strong electron-donor and electron-acceptor substituents showed significant contribution of the polarizability effect to overall solvent effect. Similar values of coefficients a and b for most **2-PY** and higher values of coefficient a with respect to b for **6-PY** (except for comp. 16) indicate different site dependent hydrogen bonding capabilities of keto/hydroxyl group. Negative values of the coefficient b indicate higher stabilization of the excited state in **2-PY** form (except comps. 11, 13, 14 and 16), while opposite is true for **6-PY** form (except comps. 2, 13 and 16, Table S10). Moreover, solvent hydrogen-bonding interactions have moderate to high contribution to the absorption maxima shift for compounds in **6-PY** form (Table S9), and preferentially act through hydrogen-bonding with the keto/hydroxyl group and the pyridine nitrogen.

The correlation results obtained for unsubstituted compound indicate highest contribution of non-specific solvent effect in **2-PY** form while highest HBA effect in **6-PY** form was found (Tables 2 and S9, respectively). Similar results were obtained according to Catalán equation (Tables 3 and S10). Larger

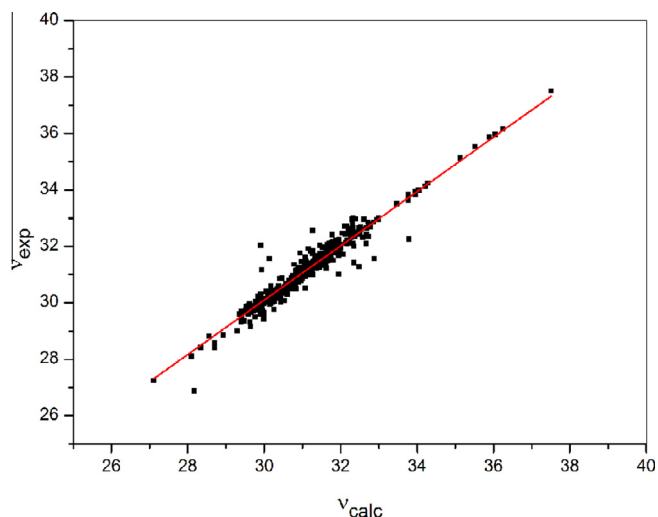


Fig. 3. The plot of ν_{exp} versus ν_{calc} .

polarizability of **2-PY** form and lower in **6-PY** form are mainly consequence of appropriate molecular adjustment which enables definite extent of π -electron conjugative transfer in the former one. Introduction of the substituents causes changes of π -electron mobility and proton-donating ability.

The success of the quantification and interpretation of solvent effects on the position of the absorption maxima of the investigated molecules was evaluated by plotting the calculated frequency (ν_{calc}), obtained by Catalán parameter set, versus the measured frequency (ν_{exp}) ($R = 0.97$, $Sd = 0.29$, $F = 7100$) (Fig. 3).

Applying described methodology [45], K_T values ($K_T = [\mathbf{6-PY}]/[\mathbf{2-PY}]$) of the investigated compounds were determined, and the results are presented in Table 4. In addition, good agreement of the presented results (Table 4) with those calculated from NMR data [25] in DMSO was obtained. The changes in the K_T values are consequence of the balanced contribution of both solvent and substituent effects. The contribution of protic solvent effects on K_T (increased contribution of HBD effect) causes shift of the tautomeric equilibria to **6-PY** form (higher K_T values); the opposite is true for aprotic solvents, *i.e.* solvent with increased dipolarity/polarizability and proton-accepting capability (lower K_T values). It could be postulated that such behavior is a consequence of the differences in conjugational ability of the π -electron densities through localized or delocalized π -electronic systems of the appropriate tautomeric forms.

Table 4
Equilibrium constants K_T of the investigated pyridones in selected solvents.

Solvent/Comp.	$\nu_{\text{max}} \times 10^{-3} (\text{cm}^{-1})$															
	1	2	3	4	5	6	7	8	9	10	11	12	13	14	15	16
Ethanol	0.51	1.99	0.13	0.83	2.01	1.33	1.53	1.87	0.33	2.47	22.1	1.04	1.50	1.07	1.18	1.68
Methanol	0.44	0.76	0.22	0.28	3.95	1.84	1.02	0.75	0.72	0.51	34.4	1.78	1.70	1.43	0.83	1.26
2-Propanol	3.53	1.63	2.39	2.54	2.97	1.17	1.39	1.49	1.73	3.87	21.2	1.17	2.02	1.12	0.73	0.86
1-Propanol	2.36	1.32	1.49	0.42	0.42	1.27	0.93	0.59	0.51	1.94	11.1	1.11	0.82	0.97	1.06	1.14
1-Butanol	1.57	1.24	1.51	3.69	3.17	0.99	1.16	1.01	1.18	3.73	8.2	1.52	1.62	1.78	1.65	0.83
2-Butanol	0.18	1.67	0.46	0.24	1.67	0.82	1.33	0.49	0.46	2.65	9.6	1.27	0.72	1.32	1.63	0.87
DMSO	1.41	0.42	0.46	2.38	0.35	^a	0.34	0.46	0.62	1.23	54.6	1.23	1.13	0.40	2.77	1.44
THF	3.63	3.12	3.02	2.06	0.50	1.21	1.27	1.18	1.23	3.91	18.7	2.08	0.57	1.04	2.69	1.71
AcN	1.24	0.67	0.55	5.72	0.87	2.75	2.23	0.78	0.76	1.00	26.5	0.95	0.80	0.39	2.11	1.08
Anisole	2.30	1.51	1.59	1.51	1.00	0.95	2.01	1.72	1.43	1.20	48.6	0.92	0.83	3.03	2.83	1.00
DMAc	0.57	1.43	1.66	0.74	1.23	-	1.56	0.89	0.84	0.68	328.1	1.09	0.71	1.08	2.06	0.85
DMF	2.71	1.13	0.47	1.23	1.32	-	0.78	0.37	0.63	0.80	420.3	1.86	0.69	0.92	1.06	5.27
EtAc	1.13	0.61	1.98	4.42	1.50	1.05	1.02	0.96	1.18	1.01	12.6	2.52	2.13	1.05	1.64	1.31
Chl	1.12	0.62	0.52	4.88	0.77	2.34	2.04	0.90	0.81	0.88	32.1	0.87	0.77	0.32	2.01	0.99
Dioxane	4.22	2.98	3.21	2.44	0.44	1.32	1.33	1.30	1.30	3.63	15.2	2.11	1.73	0.92	2.28	1.38
DEE	2.21	1.42	1.89	2.06	0.54	1.22	1.06	1.22	1.12	2.45	6.2	1.28	1.26	1.08	1.77	1.47

^a Tautomer **2-PY** exists in solution ($K_T \approx 0$).

However, surprisingly few LSER studies of tautomerism have been published on pyridones. Recently, Antonov et al. have published a paper [49] concerning tautomerism of the Schiff bases and related azo compounds which include data in a variety of solvents that have proved to be suitable for LSER study by correlating $\log K_T$ values with Kamlet-Taft solvent parameter set. Additionally, another advantage of LSER study is its ability to allow cross-comparison between the behavior of different chemical classes. The results of LSER correlation analysis using both Kamlet-Taft and Catalán set of solvent parameters are presented in Tables S13 and S14, respectively. The results display significant negative terms s , except positive found for compounds **4–6**, **11**, **15** and **16** (Table S13) related to solvent dipolarity/polarizability. Negative coefficients s identify the **2-PY** form as the more polar and the greatest negative values of s are observed for compounds **3** and **11**. Similar results were obtained according to Catalán equation.

In order to investigate the influence of the substituent electronic effects to tautomeric equilibria, $\log K_T$ values were correlated with substituent constants, σ_p , and the results are presented in Table S15. Generally, with increasing electron-accepting ability of the substituent, tautomeric equilibria is shifted to **6-PY** form. The correlation analysis of the substituent effect on tautomeric equilibria pointed out that there are two different trends involving two groups of substituents (Table S15). The first group includes electron-donating substituents and CF_3 substituent that exhibits somewhat unusual behavior and unexpectedly high $\log K_T$ value and the highest term concerning solvent polarity, *i.e.* solvent polarizability (Tables S13 and S14). The most pronounced π -electron polarizability originates from strong electron-accepting character of three fluoro atoms, and thus high susceptibility to solvent polarizability of compound **11** is a consequence. The second group of substituents contains mostly electron-accepting substituents and halogens, and also other substituents with weak electronic effects that can be placed in one or another group depending on solvent influence.

LFER analysis of UV data

A comprehensive analysis of substituent effects on absorption spectra of the investigated molecules, by using LFER principles in the form of the Hammett equation (Eq. (3)), was performed. The correlation results for **2-PY** and **6-PY** forms are given in Tables 5 and S16, respectively.

To explain substituent effects on electronic absorption spectra of the investigated pyridones, the ν_{\max} of the unsubstituted compound **1** in used solvents was taken as the reference. The LFER results indicate complex influences of both solvent and substituent effect on UV–Vis absorption maxima of both forms (Tables 5 and S16). The correlation results (Table 5), classified in the eight sets of solvents, and three groups (columns) of substituent-dependent correlation results, reflect the complex and balanced interplay of solvent and substituent electronic effects on tautomeric absorption maxima shifts. Similar results were found for compounds in **6-PY** form (Table S16).

In the two sets of protic solvents and three set of aprotic solvents, except DMAc (first column; Table 5), negative correlation slopes were obtained. Somewhat higher sensitivity of ν_{\max} to substituent effect was found for protic solvents. In the third (AcN, THF) and fourth set of solvents (Chl, Anisol), and DMAc negative solvatochromism was noticed with respect to substituent effects. Somewhat higher values and similar trend of correlation slope were found for second column, except DMSO, indicating the significance of the solvent dipolarity/polarizability and hydrogen-bonding ability to higher stabilization of excited states. Results presented in the third column indicate high sensitivity of ν_{\max} to substituent effect in aprotic solvents (AcN, THF, Chl and Anisol). In the second set of protic solvents contribution of aliphatic alcohol residue plays a significant role in the stabilization of ground state of compounds **6**, **10** and **14**.

Generally, results of LFER study show better stabilization of both forms in the excited state in protic solvents. Lower sensitivities of absorption frequencies to substituent effects in aprotic solvents can be explained by the effect of high relative permittivity of surrounding medium which causes that the energies necessary to bring about charge separation in the ground and excited state are relatively similar, which gives rise to a lower susceptibility to electronic substituent effects. Dipolar aprotic solvents behave as poor anion solvators, while they usually better stabilize larger and more dispersible positive charges. The electronic systems of the investigated pyridones, considering their *non*-planarity, could be more susceptible to the substituent influence. Study of the transmission of substituent electronic effects through defined π -resonance units of investigated compounds showed contribution of the transmission of electronic effect through isolated π -electronic unit and overall conjugated system, and their ratio depend on substitution pattern under consideration.

LFER analysis of NMR data

A comprehensive analysis of the ^{13}C NMR chemical shifts has been performed to get a better insight into transmission mode of substituent effect. The experimental and calculated ^{13}C NMR chemical shifts of the corresponding carbon atoms are given in Tables S4 and S5. The differentiation in ^{13}C NMR chemical shifts is less than 8 ppm. The general conclusion derived from the data in Tables S4 and S5 indicates that all substituents from the *N*(1)-phenyl ring influence SCS values of the carbon atoms of interest (C_1 , C_2 – C_6) via their electronic effects. The effective transmission of substituent effects, *i.e.* differences in SCS values, is affected by the conformational (geometry) change of the investigated molecules which stems from an out-of-plane rotation of the *N*(1)-phenyl ring, *i.e.* defined by the torsion angle θ values (Fig. 1). Optimized geometries were calculated by the use of B3LYP functional with 6-311G(d,p) basis set (Tables S17 and S18) [25].

The analysis of the substituent effect on the SCS of the carbon atoms of interest, performed by the use of LFER's Eq. (3) (*i.e.* SSP) with σ or σ^+ substituent constants have been applied, and the correlation results obtained for C_1 , C_2 – C_6 carbons are presented in Tables 6 and S19.

The observed ρ values indicate different susceptibilities of the SCS to substituent effects. It can be noticed from Tables 6 and S19 that correlations are of good to high quality which means that the SCS values reflect electronic substituent effects. It is apparent that chemical shifts of C_1 show an increased susceptibility and normal substituent effect. Reverse substituent effect was observed at C_2 for *para*-substituents, as well as for C_3 and C_4 atoms (Table 6). The negative sign of reaction constant, ρ , means reverse behavior, *i.e.* the value of SCS decreases although the electron-withdrawing ability of the substituents, measured by σ , increases. The reverse substituent effect at C_2 (for *para*-substituents), C_3 and C_4 atoms can be attributed to localized π -polarization [50], which predominates over the extended π -polarization (Table 6) in the compounds in **2-PY** form. Correlations for C_1 carbon are slightly improved when electrophilic substituent constants σ^+ are used (second line; Table 6), which indicates that contribution of extended resonance interaction, *i.e.* more intensive interaction of electron-donating substituent with electrophilic C_1 carbon, is operative within phenyl ring. The SCS of C_6 showed nonlinear (parabolic) dependence with respect to substituent effect. Similar results were found for compounds in **6-PY** form (Table S19), except normal substituent effect found for C_2 carbon.

To measure separate contributions of the polar (inductive/field) and resonance effects of substituent, the regression analysis according to DSP Eq. (4) with σ_1 and σ_R constants has been performed, and the results are given in Tables 7 and S20. The DSP equation does not provide significant improvement in fits when compared to the results of SSP Eq. (1). The positive ρ_1 and ρ_R values have been obtained for the C_1 , C_2 (3-sub. comps.), C_3 and C_5 atoms, while the negative values have been found for C_2 (comps. **1**, **2**, **3**, **6** and **10**) and C_4 confirming that reverse substituent effect is operative at these carbons. All the τ values are higher than 1, except for C_5 carbon, which means that resonance substituent effect predominates over field effect, and the most pronounced is at C_4 . The resonance interaction significantly depends on spatial arrangement of the molecules, *i.e.* the values of torsional angle θ , and thus, the resonance substituent effect is most effectively transmitted to C_1 and C_4 carbons, *i.e.* C_4 is *para*-position of the carbon of pyridone ring with respect to *N*-substituted phenyl ring.

Comparative analysis of the structural effect of the substituent at C_6 position: OH group in compounds in **2-PY** form and methyl group in a series of *N*(1)-(4-substituted phenyl)-3-cyano-4,6-dimethyl-2-pyridones [51] could give some additional information on structural effect, the mode and extent of transmission of substituent effect.

On the basis of the sign of the constants ρ for investigated compounds (Table 7) and from the literature data for *N*(1)-(4-substituted phenyl)-3-cyano-4,6-dimethyl-2-pyridones [51], similar behavior was found for C_1 and C_5 , while positive and significantly lower proportionality constants for C_2 and C_3 atoms were obtained [51]. The highest influence of substituent effects is observed at C_1 carbon for investigate compounds in **2-PY** form and also highest and somewhat lower values were found for *N*(1)-(4-substituted phenyl)-3-cyano-4,6-dimethyl-2-pyridones. Higher values of correlation coefficients for C_3 and C_5 carbons indicate the significance of electron-donating capability of hydroxyl group at C_6 carbon, in comparison to low hyperconjugative character of methyl group.

DFT, TD-DFT and Bader's analysis. Evaluation of electronic transition and charge density change

An additional analysis of solvent and substituent effects on absorption frequencies, tautomeric equilibria and conformational changes of the studied compounds, necessitated quantum-chemical calculations, *i.e.* geometry optimization and charge

Table 5
Regression fits according to Eq. (3) for the 2-PY form.

	$\nu_0 \times 10^{-3}$ (cm^{-1})	$\rho \times 10^{-3}$ (cm^{-1})	<i>R</i>	<i>Sd</i>	<i>F</i>	$\nu_0 \times 10^{-3}$ (cm^{-1})	$\rho \times 10^{-3}$ (cm^{-1})	<i>R</i>	<i>Sd</i>	<i>F</i>	$\nu_0 \times 10^{-3}$ (cm^{-1})	$\rho \times 10^{-3}$ (cm^{-1})	<i>R</i>	<i>Sd</i>	<i>F</i>
	2, 3, 15					1, 7, 10, 14					9, 12, 13, 16				
Methanol	30.07 ± 0.06	−4.45 ± 0.32	0.99	0.04	196.39	31.57 ± 0.02	−5.93 ± 0.23	0.99	0.03	660.08	32.58 ± 0.69	−5.89 ± 1.99	0.90	0.26	8.79
Ethanol	30.50 ± 0.15	−1.55 ± 0.78	0.90	0.11	3.95	31.31 ± 0.08	−4.52 ± 0.71	0.98	0.09	40.20	32.05 ± 0.24	−4.72 ± 0.68	0.98	0.09	43.38
	1, 4, 7, 8, 9, 12, 13, 14					2, 3, 15					6, 10, 14				
1-Propanol	31.25 ± 0.15	−3.38 ± 0.41	0.95	0.26	68.89	30.37 ± 0.06	−1.55 ± 0.32	0.98	0.04	23.83	30.89 ± 0.03	2.08 ± 0.14	0.99	0.05	1.77
2-Propanol	31.49 ± 0.18	−3.67 ± 0.49	0.94	0.31	56.07	30.24 ± 0.33	−2.65 ± 1.76	0.83	0.25	2.26	30.80 ± 0.22	1.27 ± 0.95	0.80	0.36	217.90
1-Butanol	31.27 ± 0.14	−3.35 ± 0.39	0.95	0.25	73.12	28.88 ± 0.41	−8.55 ± 2.16	0.97	0.31	15.59	30.79 ± 0.17	1.00 ± 0.75	0.80	0.28	1.78
2-Butanol	31.25 ± 0.14	−3.47 ± 0.38	0.96	0.24	81.76	29.79 ± 0.17	−4.15 ± 0.89	0.98	0.13	21.50	30.71 ± 0.14	1.29 ± 0.62	0.90	0.23	4.37
	2, 5, 6, 9, 14					4, 7, 8, 11					12, 13, 16				
AcN	30.45 ± 0.09	1.18 ± 0.29	0.92	0.20	16.93	29.67 ± 0.11	2.43 ± 0.34	0.97	0.22	50.10	33.79 ± 0.66	−10.00 ± 1.73	0.98	0.02	33.33
THF	30.59 ± 0.04	1.54 ± 0.14	0.99	0.09	122.12	29.97 ± 0.09	1.59 ± 0.22	0.97	0.14	49.96	22.39 ± 1.32	20.00 ± 3.46	0.98	0.05	33.33
	2, 5, 6, 9					4, 7, 8, 11, 15					12, 13, 16				
Chl	30.95 ± 0.13	0.87 ± 0.37	0.85	0.25	5.46	30.66 ± 0.11	1.64 ± 0.25	0.98	0.16	41.22	24.81 ± 8.67	14.7 ± 8.8	0.54	0.32	0.64
Anisol	30.90 ± 0.07	0.58 ± 0.21	0.89	0.14	7.45	30.27 ± 0.25	1.15 ± 0.60	0.74	0.38	3.66	52.24 ± 12.40	−59.5 ± 32.62	0.88	0.46	3.33
	2, 3, 7, 12, 13, 14, 15					1, 8, 9, 10, 16					4, 5, 6				
EtAc	30.44 ± 0.08	−1.76 ± 0.34	0.92	0.22	26.58	31.40 ± 0.04	−3.81 ± 0.20	0.99	0.06	358.16	30.61 ± 0.05	1.52 ± 0.08	0.99	0.07	343.95
Dioxane	30.42 ± 0.08	−2.10 ± 0.33	0.94	0.21	41.26	31.46 ± 0.08	−3.15 ± 0.37	0.98	0.11	73.15	30.55 ± 0.28	1.15 ± 0.48	0.92	0.41	5.70
DEE	30.46 ± 0.06	−2.66 ± 0.23	0.98	0.14	133.25	31.57 ± 0.14	−3.67 ± 0.62	0.96	0.19	34.69	30.61 ± 0.41	0.96 ± 0.71	0.80	0.60	1.82
	5, 7, 8, 9, 12, 13, 16					3, 6, 14, 15					1, 2, 10				
DMSO	29.47 ± 0.08	−0.95 ± 0.23	0.88	0.06	16.66	30.39 ± 0.04	2.45 ± 0.15	0.99	0.06	248.92	29.95 ± 0.01	1.25 ± 0.02	0.99	0.01	3830.6
	1, 2, 3, 5, 10, 11, 15, 16					4, 7, 8, 16					3, 6, 9				
DMAc	30.48 ± 0.08	1.76 ± 0.27	0.94	0.22	42.62	29.50 ± 0.04	1.35 ± 0.09	0.99	0.04	221.06	30.02 ± 0.01	1.18 ± 0.02	0.99	0.01	4973.75
	1, 2, 9, 11, 13, 14					7, 10, 12, 16					2, 4, 6				
DMF	30.06 ± 0.04	−2.16 ± 0.16	0.99	0.07	182.97	29.87 ± 0.04	−2.27 ± 0.15	0.99	0.09	219.24	29.44 ± 1.41	−1.70 ± 2.46	0.57	2.08	0.48

Table 6Correlation results of the SCS values of **2-PY** tautomer with σ_p/σ_m and σ_p^+/σ_m^+ substituent constants using Hammett Eq. (3).

		ρ	h	R	F	Sd	n	Included
C ₁	σ	13.76 ± 1.59	-2.20 ± 0.53	0.923	75	1.83	15	All
	σ^+	9.45 ± 0.92	-0.53 ± 0.41	0.943	105	1.58	15	All
	σ^-	10.05 ± 1.43	-2.08 ± 0.52	0.925	77	1.80	15	All
	σ	15.32 ± 1.58	-2.41 ± 0.56	0.960	94	1.66	10	4-Substituted ^a
	σ^+	10.30 ± 0.98	-0.22 ± 0.49	0.966	111	1.53	10	4-Substituted
	σ	16.62 ± 0.87	-3.26 ± 0.34	0.992	368	0.86	8	4-(H i Me excluded)
	σ^+	8.91 ± 0.41	0.70 ± 0.24	0.992	476	0.76	8	4-(H i Me excluded), σ_p^- (NO ₂)
	σ	3.70 ± 1.00	0.20 ± 0.27	0.880	14	0.46	6	3-Substituted ^b
	σ^+	3.36 ± 1.00	0.28 ± 0.28	0.860	11	0.50	6	3-Substituted
	σ	4.58 ± 0.46	0.20 ± 0.11	0.985	99	1.93	5	3-(COMe excluded)
	σ^+	3.73 ± 0.81	0.44 ± 0.24	0.956	21	0.34	5	3-(COMe excluded)
C ₂	σ	-1.70 ± 0.17	0.02 ± 0.04	0.985	96	0.06	5	H, OH, OMe, Me, F
	σ^+	-0.37 ± 0.05	0.26 ± 0.03	0.967	58	0.06	6	OH, OMe, Me, Cl, Br, COMe
	σ	1.13 ± 0.21	0.03 ± 0.06	0.936	28	0.10	6	3-substituted
	σ	0.95 ± 0.09	0.02 ± 0.02	0.988	28	0.04	5	H, 3-Br, 3-OMe, 3-Me, 3-COMe
C ₃	σ	-1.94 ± 0.16	0.18 ± 0.04	0.975	156	0.13	10	H, OH, OMe, Me, Cl, Br, I, COMe, 3-Br, 3-Me
	σ^+	-1.17 ± 0.12	-0.04 ± 0.05	0.954	104	0.16	10	H, OH, OMe, Me, Cl, Br, I, COMe, 3-Br, 3-Me
C ₄	σ	-0.64 ± 0.12	0.10 ± 0.03	0.912	30	0.08	8	H, OH, OMe, Me, F, I, COMe, 3-Me
	σ	-0.80 ± 0.15	0.51 ± 0.06	0.938	29	0.08	6	NO ₂ , Cl, Br, 3-Cl, 3-Br, 3-OMe
C ₅	σ^+	0.55 ± 0.05	0.38 ± 0.03	0.965	109	0.08	10	OH, OMe, Me, F, Cl, Br, COMe, 3-Br, 3-Cl, 3-OMe
C ₆	σ	(1.31 ± 0.31) σ^2	(-0.65 ± 0.18) σ	0.926	9	0.08	6	H, OH, F, I, COMe, NO ₂
	σ	(4.79 ± 0.72) σ^2	(-0.89 ± 0.17) σ	0.958	22	0.08	7	Me, OMe, 3-Cl, 3-Br, 3-OMe, 3-Me, 3-COMe

^a All 4-substituted compounds.^b All 3-substituted compounds.**Table 7**Correlation results of the SCS values of **2-PY** tautomer with σ_I and σ_R substituent constants using Eq. (4).

Atom		ρ_I	ρ_R	h	R	τ^a	F	Sd	n	Included
C ₁	σ	8.47 ± 1.92	17.13 ± 1.59	0.13 ± 0.78	0.956	2.02	63	1.45	15	All
	σ	9.66 ± 1.98	18.25 ± 1.57	0.17 ± 0.85	0.979	1.89	82	1.28	10	4-Substituted ^b
	σ	9.75 ± 5.43	18.26 ± 2.38	0.14 ± 2.70	0.982	1.87	58	1.51	8	4-sub. (H i Me excluded)
	σ	3.84 ± 0.78	0.22 ± 2.00	-0.05 ± 0.25	0.947	0.06	13	0.36	6	3-Substituted ^c
	σ	4.48 ± 0.23	2.64 ± 0.65	0.07 ± 0.07	0.998	0.59	208	0.10	5	3-sub. (COMe excluded)
C ₂	σ	-1.31 ± 0.34	-1.30 ± 0.26	0.08 ± 0.09	0.963	0.99	13	0.12	5	H, OH, OMe, Me, F
	σ	1.12 ± 0.25	1.22 ± 0.63	0.03 ± 0.08	0.936	1.09	11	0.11	6	3-Substituted
	σ	0.94 ± 0.09	1.12 ± 0.21	0.04 ± 0.03	0.992	1.19	59	0.04	5	H, 3-Br, 3-OMe, 3-Me, 3-COMe
C ₃	σ	1.56 ± 0.31	-2.06 ± 0.26	0.02 ± 0.10	0.957	1.32	38	0.19	10	H, OH, OMe, Me, Cl, Br, I, COMe, 3-Br, 3-Me
C ₄	σ	-0.55 ± 0.24	-0.62 ± 0.18	0.08 ± 0.06	0.850	1.13	7	0.12	8	H, OH, OMe, Me, F, I, COMe, 3-Me
	σ	-0.15 ± 0.74	-1.22 ± 0.51	0.18 ± 0.39	0.945	8.13	12	0.08	6	NO ₂ , Cl, Br, 3-Cl, 3-Br, 3-OMe
C ₅	σ	2.42 ± 0.76	1.92 ± 0.67	0.02 ± 0.31	0.779	0.79	9	0.57	15	all
	σ	2.65 ± 1.02	2.04 ± 0.81	0.10 ± 0.44	0.813	0.77	7	0.66	10	4-substituted
	σ	0.97 ± 0.24	0.83 ± 0.18	0.17 ± 0.09	0.898	0.86	17	0.13	11	H, OH, OMe, Me, Cl, Br, I, COMe, 3-Br, 3-Me, 3-OMe
	σ	1.80 ± 0.44	4.16 ± 1.04	0.16 ± 0.17	0.965	2.31	14	0.17	5	3-substituted

^a $\tau = \rho_R/\rho_I$.^b All 4-substituted compounds.^c All 3-substituted compounds.

density analysis were performed. Geometry optimization of the investigated molecules was performed by the use of B3LYP functional with 6-311G(d,p) basis set. The most stable conformations of compounds **1–16** (with exception of compound **7**) in **2-PY** and **6-PY** forms are presented in Figs. S6 and S7, respectively. Elements of optimized geometries of calculated compounds are given in Tables S17 and S18.

The calculation of optimal geometry, with focus on determination of the value of torsion angle θ (Fig. 1), gives valuable results required for better understanding of the transmission of substituent effects, i.e. electron density distribution. More planar molecule, i.e. molecule with lower torsional angle, induces red shift in the absorption spectra [25]. In the investigated molecules these values are fairly similar and mostly depend on substituent present. Somewhat larger differences of θ was noticed for electron-donor substituted compounds (Tables S17 and S18: 80.18 for compound

2 in **2-PY** form and 82.77 for compound **14** in **6-PY** form), indicating significance of extended resonance interaction in electron-donor substituted compounds. Oppositely, in electron-acceptor substituted compounds appropriate contribution of n,π -conjugation (nitrogen lone pair participation) to overall electronic interaction with π -electronic system of pyridone unit causing perturbation of π -electron density.

The results shown in Tables S17 and S18 indicate that bond lengths of **2-PY** and **6-PY** forms are obviously different and there is similar alteration of the values with respect to form under consideration. Some values of bond distances are in the frame of statistical errors and thus they are not suitable for evaluation purpose. In general, low influences of electronic substituent effects could be noticed. Since the TD-DFT results have indicated a large contribution of single particle HOMO to LUMO excitations in ground to first excited state transition (greater than 80% for all

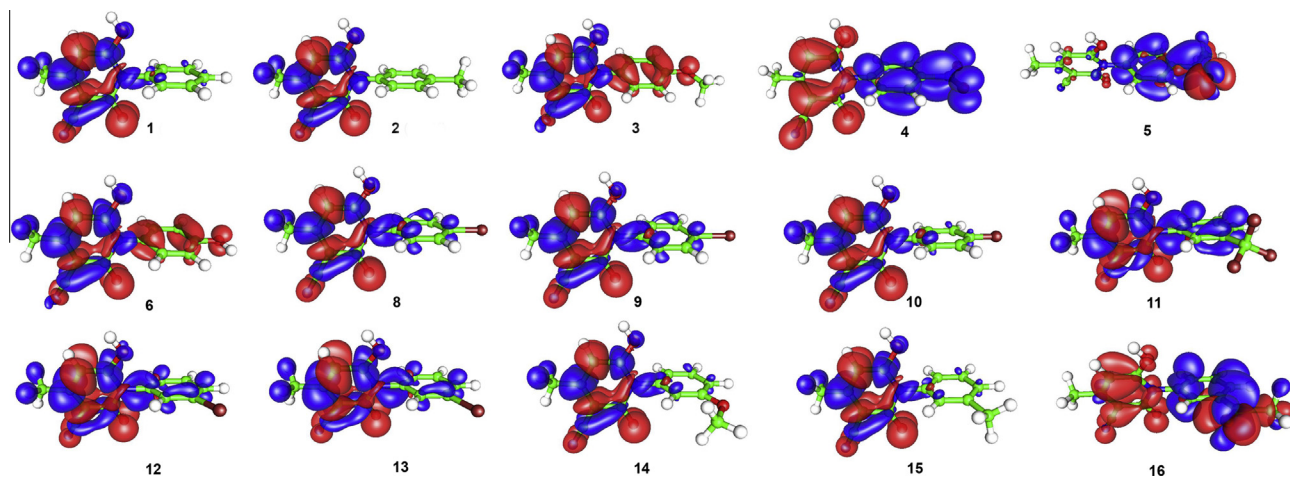


Fig. 4. ICT processes from ground state (red) to excited state (blue) of compounds **1–16** in **2-PY** form. (For interpretation of the references to colour in this figure legend, the reader is referred to the web version of this article.)

calculated compounds, except for **6-PY** form of compound **16**, [Tables S6 and S7](#)), mechanism of electronic excitations and the electron density distribution in ground and excited states can be studied by calculation of HOMO/LUMO energies ($E_{\text{HOMO}}/E_{\text{LUMO}}$) and E_{gap} values ([Tables S21 and S22](#), and [Fig. S8–S11](#)). In conclusion, a lower E_{gap} values were observed for all compounds in **2-PY** form, and the lowest values were found for nitro-substituted compound, which is consistent with largest bathochromic shift. Concerning electron-donor substituents, small influences on E_{gap} changes could be observed. For compounds **1–16** in **6-PY** form ([Table S22](#)), the substituent effects influence E_{gap} changes displaying similar trend as for compounds in **2-PY** form. Additional discussion on TD-DFT results is given in [Supplementary material](#) (pages 37 and 38). In order to obtain data on electronic density distribution, the Bader's charge analysis was performed. Bader's theory of atoms in molecules is useful to define the charge enclosed within the Bader volume as a good approximation of the total electronic charge of an atom. Atom and ring numbering used in Bader's analysis is given in [Fig. S12](#). Difference of atomic charges in the excited and in the ground state (Δ_{charge}) for appropriate atoms, as well as calculated changes in overall electron density of molecules are given in [Tables S23–S27](#), and [Figs. 4 and S13](#).

According to the results shown in [Tables S23–S27](#) and [Figs. 4 and S13](#), it could be observed that in both **2-PY** and **6-PY** forms nitro-substituted compounds **4** exhibit distinct ICT processes. Electron density was transferred from the pyridone ring to the substituted phenyl. According to the character of the ICT processes, molecules can be divided in three groups:

The first group includes compounds **1, 2, 8–10, 14, 15** in **2-PY** form ([Fig. 4](#)), along with **1–3, 6, 14 and 15** in **6-PY** compound ([Fig. S13](#)). In these molecules no observable ICT process was found, and electron density was concentrated on pyridone moieties in both ground and excited states: moderate Δ_{charge} for the pyridone ring vary from -0.0056 to -0.0625 in **2-PY** form and from -0.0022 to -0.0661 in **6-PY** form. Along with this, carbonyl O_{13} atom of the pyridone ring loses a significant amount of charge (Δ_{charge}): from -0.039 to -0.2219 for compounds in **2-PY** form, while in **6-PY** form non-consistent alteration at carbonyl O_{15} atom was found. Exception is compound **5** in **2-PY** form and compounds **5 and 16** in **6-PY** form where low extent of ICT is operative with mostly observable Δ_{charge} at substituted phenyl ring.

In the second group, which includes compounds **4 and 16** in **2-PY** and compounds **4** (strong), while in compounds **8, 9** and

11–13 in **6-PY**, ICT process is less pronounced. The calculation showed that pyridone moiety of compounds **4** and **16** loses -0.9346 and -0.4468 electrons, while nitro- and acetyl-substituted phenyl ring receives 0.9438 and 0.4466 electrons, respectively. Along with this, O_{13} carbonyl oxygen of the pyridone ring loses low amount of charge (Δ_{charge}): -0.1917 for comp. **4** and -0.1068 for comp. **16**). Similar result was found for compound **4** in **6-PY** form: Δ_{charge} shows loses from pyridone is -0.9384 and nitro substituted phenyl ring receives 0.9381 electron.

In the third group, compounds **3** and **6** in **2-PY** form shows moderate ICT which occurs from methoxy- and hydroxy-substituted phenyl to pyridone ring with Δ_{charge} -0.2438 and -0.1622 , and pyridone ring receives 0.2439 and 0.1617 electrons, respectively ([Table S27](#)). Observed charge transfer can be explained by resonance effect of compounds **3** and **6**, bearing electron-donating, moderate, methoxy- and, strong, hydroxy-substituent. It should be noted that in hydroxy-substituted compound charge difference between the ground and the excited state is lower than in compound **3**, which means that significantly higher proton-donating capabilities of hydroxy group contribute to lower polarizability of π -electron density.

Conclusions

Tautomeric equilibria of 2(6)-hydroxy-4-methyl-6(2)-oxo-1-(substituted phenyl)-1,2(1,6)-dihydropyridine-3-carbonitriles were qualitatively/quantitatively analyzed by UV-Vis spectroscopy and quantum chemical calculations. Results of LSER analysis imply that negative sign of coefficients s and b indicate better stabilization of the molecule in the ground state for compounds in **2-PY** form, while the opposite is true for HBD solvent effect. On the contrary, most of compounds in **6-PY** form display a hypsochromic shift with increasing solvent dipolarity/polarizability and hydrogen-accepting capability.

The tautomeric constants K_T were estimated by using an advanced spectral data processing method based on resolution of overlapping bands. The study of solvent influence on tautomeric equilibria showed high contribution of solvent dipolarity/polarizability, *i.e.* the negative s term indicates that increasing solvent polarity favors **2-PY** tautomer. The analysis of the substituent effect on K_T change shows that increasing electron-accepting ability of the substituents shifts tautomeric equilibria to **6-PY** form.

The LFER analysis applied on ν_{max} implies that solvent effects have significant influence on the transmission mode of substituent

effects. Positive solvatochromism was found mainly for protic solvents. The LFER analysis of SCS data for C₁ shows the largest and normal substituent effect. Reverse substituent effect was observed at C₂ for *para*-substituents, as well as for C₃ and C₄ atoms for compounds in **2-PY** form. Similar results were found for compounds in **6-PY** form. The correlation results for SCS values of C₆ showed nonlinear (parabolic) dependence on substituent constants.

Quantum chemical calculations of the optimal geometries of both tautomeric forms were performed by the use of B3LYP functional with 6-311G(d,p) basis set. The inclusion of solvent effects and the TD-DFT calculations demonstrated that substituents, depending on their position in molecules, significantly change the conjugation extent, and further affect the ICT character of the investigated pyridones. In addition, Bader's analysis showed that similar processes of electronic excitation are operative in both **2-PY** and **6-PY** forms. In *nitro*-substituted compound a distinct ICT was noticed and moderate process in halogen substituted compound in **6-PY** form.

Acknowledgement

This work was supported by the Ministry of Education, Science and Technological Development of the Republic of Serbia (Project 172013).

Appendix A. Supplementary data

Supplementary data associated with this article can be found, in the online version, at <http://dx.doi.org/10.1016/j.saa.2015.05.055>.

References

- [1] D.Ž. Mijin, J.M. Marković, D.V. Brković, A.D. Marinković, *Hem. Ind.* 68 (2014) 1–14.
- [2] D.Ž. Mijin, G.S. Ušćumlić, N.V. Valentić, A.D. Marinković, *Hem. Ind.* 65 (2011) 517–532.
- [3] L. Antonov, *Tautomerism: Methods and Theories*, Wiley-VCH, Weinheim, 2013.
- [4] C. Altomare, S. Cellamare, L. Summo, P. Fossa, L. Mosti, A. Carotti, *Bioorg. Med. Chem.* 8 (2000) 909–916.
- [5] N. Trišović, N. Valentić, M. Erović, T. Đaković-Sekulić, G. Ušćumlić, I. Juranić, *Monatsh. Chem.* 142 (2011) 1227–1234.
- [6] A.S.A. Alimmari, B.D. Bozic, A.D. Marinković, D.Ž. Mijin, G.S. Ušćumlić, *J. Solution Chem.* 41 (2012) 1825–1835.
- [7] L. Forlani, G. Cristoni, C. Boga, P.E. Todesco, E. Del Vecchio, S. Selva, M. Monari, *ARKIVOC* 11 (2002) 198–215.
- [8] M.J. Nowak, L. Lapinski, J. Fulara, A. Les, L. Adamowicz, *J. Phys. Chem.* 96 (1992) 1562–1569.
- [9] C.S. Peng, A. Tokmakoff, *J. Phys. Chem. Lett.* 3 (2012) 3302–3306.
- [10] H.I. Abdulla, M.F. El-Bermani, *Spectrochim. Acta, Part A* 57 (2001) 2659–2671.
- [11] J. Seliger, V. Zagar, *J. Phys. Chem. A* 117 (2013) 1651–1658.
- [12] C. Lopez, R.M. Claramunt, I. Alkorta, J. Elguero, *Spectroscopy (Amsterdam)* 14 (2000) 121–126.
- [13] D.G. De Kowalewski, R.H. Contreras, E. Diez, A. Esteban, *Mol. Phys.* 102 (2004) 2607–2615.
- [14] P. Beak, F.S. Fry, *J. Am. Chem. Soc.* 95 (1973) 1700–1702.
- [15] L.D. Hatherley, R.D. Brown, P.D. Godfrey, A.P. Pierlot, W. Caminati, D. Damiani, S. Melandri, L.B. Favero, *J. Phys. Chem.* 97 (1993) 46–51.
- [16] A. Les, L. Adamowicz, M.J. Nowak, L. Lapinski, *J. Mol. Struct.: Theochem.* 96 (1992) 313–327.
- [17] M. Ben Messaouda, M. Abderrabba, A. Mahjoub, G. Chambaud, M. Hochlaf, *Comput. Theor. Chem.* 990 (2012) 94–99.
- [18] G. Galstyan, E.W. Knapp, *J. Phys. Chem. A* 116 (2012) 6885–6893.
- [19] T.L.P. Galvao, I.M. Rocha, M.D.M.C. Ribeiro da Silva, S. Ribeiroda, A.V. Manuel, *J. Phys. Chem. A* 117 (2013) 12668–12674.
- [20] A. Kvick, *Acta Crystallogr. Sect. B* 32 (1976) 220–224.
- [21] H.W. Yang, R.M. Craven, *Acta Crystallogr. Sect. B: Struct. Sci.* 54 (1998) 912–920.
- [22] G. Ramirez-Galicia, G. Perez-Caballero, M. Rubio, *J. Mol. Struct.: Theochem.* 542 (2001) 1–6.
- [23] A. Dkhissi, L. Houben, J. Smets, L. Adamowicz, G. Maes, *J. Mol. Struct.* 484 (1999) 215–227.
- [24] H.B. Schlegel, P. Gund, E.M. Fluders, *J. Am. Chem. Soc.* 104 (1982) 5347–5351.
- [25] I. Ajaj, D. Mijin, V. Maslak, D. Brković, M. Milčić, N. Todorović, A. Marinković, *Monatsh. Chem.* 144 (2013) 665–675.
- [26] M.J. Kamlet, J.L.M. Abboud, R.W. Taft, An examination of linear solvation energy relationships, in: R.W. Taft (Ed.), *Progress in Physical Organic Chemistry*, vol. 13, Wiley, New York, 1981, pp. 485–630.
- [27] J. Catalan, *J. Phys. Chem. B* 113 (2009) 5951–5960.
- [28] M. Rančić, N. Trišović, M. Milčić, G. Ušćumlić, A. Marinković, *Spectrochim. Acta A* 86 (2012) 500–507.
- [29] (a) O. Exner, The Hammett Equation – the Present Position, *Advances in Linear Free Energy Relationship*, N. B. Chappan and J. Shorter (Eds.), Plenum Press, London (1972) pp. 1–69.;
(b) C. Hansch, A. Leo, D. Hoekman, *Exploring QSAR: Hydrophobic, Electronic and Steric Constants*; American Chemical Society, ACS Professional Reference Book, American Chemical Society, Washington, DC, 1995.
- [30] Y. Tsuno, Y. Kusuyama, M. Sawada, T. Fuji, Y. Yukawa, *Bull. Chem. Soc. Jpn.* 48 (1975) 3337–3346.
- [31] L. Antonov, S. Stoyanov, *Anal. Chim. Acta* 314 (1995) 225–232.
- [32] L. Antonov, S. Stoyanov, *Appl. Spectrosc.* 47 (1993) 1030–1035.
- [33] V. Barone, A. Polimeno, *Chem. Soc. Rev.* 36 (2007) 1724–1731.
- [34] P. Wiggins, J.A.G. Williams, D.J. Tozer, *J. Chem. Phys.* 131 (2009). 091101/1-091101/4.
- [35] K.W. Wiitala, T.R. Hoye, C.J. Cramer, *J. Chem. Theory Comput.* 2 (2006) 1085–1092.
- [36] R. Jain, T. Bally, P.R. Rablen, *J. Org. Chem.* 74 (2009) 4017–4023.
- [37] Gaussian 09, Revision D.01, M.J. Frisch, G.W. Trucks, H.B. Schlegel, G.E. Scuseria, M.A. Robb, J.R. Cheeseman, G. Scalmani, V. Barone, B. Mennucci, G.A. Petersson, H. Nakatsuji, M. Caricato, X. Li, H.P. Hratchian, A.F. Izmaylov, J. Bloino, G. Zheng, J.L. Sonnenberg, M. Hada, M. Ehara, K. Toyota, R. Fukuda, J. Hasegawa, M. Ishida, T. Nakajima, Y. Honda, O. Kitao, H. Nakai, T. Vreven, J.A. Montgomery, Jr., J.E. Peralta, F. Ogliaro, M. Bearpark, J.J. Heyd, E. Brothers, K.N. Kudin, V.N. Staroverov, R. Kobayashi, J. Normand, K. Raghavachari, A. Rendell, J.C. Burant, S.S. Iyengar, J. Tomasi, M. Cossi, N. Rega, J.M. Millam, M. Klene, J.E. Knox, J.B. Cross, V. Bakken, C. Adamo, J. Jaramillo, R. Gomperts, R.E. Stratmann, O. Yazyev, A.J. Austin, R. Cammi, C. Pomelli, J.W. Ochterski, R.L. Martin, K. Morokuma, V.G. Zakrzewski, G.A. Voth, P. Salvador, J.J. Dannenberg, S. Dapprich, A.D. Daniels, Ö. Farkas, J.B. Foresman, J.V. Ortiz, J. Cioslowski, D.J. Fox, Gaussian Inc., Wallingford CT, 2009.
- [38] W. Tang, E. Sanville, G. Henkelman, *J. Phys.: Condens. Matter* 21 (2009) 084204–084210.
- [39] L. Laaksonen, *J. Mol. Graphics* 10 (1992) 33–34.
- [40] Ł. Szyc, J. Guo, M. Yang, J. Dreyer, P.M. Tolstoy, E.T.J. Nibbering, B. Czarnik-Matuszewicz, T. Elsaesser, H.H. Limbach, *J. Phys. Chem. A* 114 (2010) 7749–7760.
- [41] N. Tsuchida, S. Yamabe, *J. Phys. Chem. A* 109 (2005) 1974–1980.
- [42] E. Kolehmainen, B. Ośmiałowski, T.M. Krygowski, R. Kauppinen, M. Nissinen, R. Gawinecki, *J. Chem. Soc., Perkin Trans. 2* (2000) 1259–1266.
- [43] Y. Manolova, V. Deneva, L. Antonov, E. Drakalska, D. Mornekova, N. Lambov, *Spectrochim. Acta A* 132 (2014) 815–820.
- [44] S. Ortiz, M.C. Alvarez-Ros, M. Alcolea Palafox, V.K. Rastogi, V. Balachandran, S.K. Rathor, *Spectrochim. Acta A* 130 (2014) 653–668.
- [45] J. Dostanić, D. Mijin, G. Ušćumlić, D.M. Jovanović, M. Zlatar, D. Lončarević, *Spectrochim. Acta A* 123 (2014) 37–45.
- [46] I. Ajaj, J. Markovski, J. Marković, M. Jovanović, M. Milčić, F. Assaleh, A. Marinković, *Struct. Chem.* 25 (2014) 1257–1270.
- [47] V. Petrov, L. Antonov, H. Ehara, N. Harada, *Comput. Chem.* 24 (2000) 561–569.
- [48] C. Reichardt, *Solvents and Solvent Effect in Organic Chemistry*, Wiley-VCH Verlag GmbH & Co. KGaA, Weinheim, 2003.
- [49] L. Antonov, M.F. Fabian, P. Taylor, *J. Phys. Org. Chem.* 18 (2005) 169–175.
- [50] M. Rančić, N. Trišović, M. Milčić, I. Ajaj, A. Marinković, *J. Mol. Struct.* 1049 (2013) 59–68.
- [51] A. Marinković, N. Valentić, D. Mijin, G. Ušćumlić, B. Jovanović, *J. Serb. Chem. Soc.* 73 (2008) 513–524.